

Micro-kinetic analysis and Monte Carlo simulation in methane partial oxidation into synthesis gas

Wen-Shu Yang, Hong-Wie Xiang, Yong-Wang Li*, Yu-Han Sun

State Key Laboratory of Coal Conversion, Institute of Coal Chemistry, Chinese Academy of Science, Taiyuan, Shanxi 030001, PR China

Abstract

The mechanism outlined in literature for methane steam reforming over nickel catalysts is reviewed. Activation energy of this set of elementary steps for methane conversion into synthesis gas is obtained on the basis of bond order conservation Morse potential (BOC-MP), and the pre-exponential factors of the rate expressions of these elementary steps are then estimated according to the reported ranges in literature. A real-time Monte Carlo approach is developed to simulate the micro-kinetic trends for this catalytic process. © 2000 Elsevier Science B.V. All rights reserved.

Keywords: Methane steam reforming; Micro-kinetics; Real-time Monte Carlo; Probability

1. Introduction

The catalytic reforming of methane with steam is one of the important industrial processes in natural gas utilization [1]. Usually the catalytic process is carried out by using a catalyst consisting essentially of nickel deposited on porous refractory carrier, such as alumina or silica. The methane steam reforming consists of two major reactions, the reaction of methane with water producing hydrogen and carbon monoxide and water gas shift to carbon dioxide [2]. The catalytic investigation on this process has provided the basis of the reaction mechanism [2–6]. Detailed experimental and modeling kinetics studies have also been performed [4]. This kind of efforts provides a route to kinetically optimize the reforming reaction, which has been a classical engineering style of kinetic researches. However the kinetics providing detailed information on each elementary step, namely micro-kinetics, has

not fully been addressed, retaining the gap between the engineering kinetics and the understanding of the micro-nature of the catalytic processes. Micro-kinetics analysis proposed by Dumesic et al. [7] is one of the approaches, which has been developed to fill this gap, by fully using theoretical estimation of kinetic parameters of elementary steps.

Monte Carlo (MC) methods have frequently been used in complex kinetic simulations in recent years [8–13]. Some of them are suitable for the simulation of heterogeneous reactions, e.g., the MC approach combined with two-dimensional lattice representing catalyst surfaces is useful to describe an ensemble of catalytic sites by properly arranging the distribution of the sites on the lattice. However, the reported MC approaches have not considered either the real concentration and timescales but with arbitrary units instead for both concentration and time [12,14,15]. This work is oriented to the simulation of methane steam reforming reaction by using a real-time MC approach, in which the catalytic surface is expressed by two-dimensional square lattice with its nodes representing the catalytic

* Corresponding author. Fax: +0086-351-4050320.
E-mail address: ywl@public.ty.sx.cn (Y.-W. Li).

sites, and all the physical quantities are scaled with real units.

2. Kinetic basis for methane steam reforming

The understanding of the catalytic nature of methane reforming reactions over group VIII metals as catalysts has long been a hot topic in the catalysis field [1,16–18]. Starting from recognizing the nature of methane activation over metal surfaces, considerable advances have been made in the mechanism aspects of the catalytic methane reforming process. For methane steam reforming over nickel catalysts, several common points, although some are still in debate, may be summarized: (1) methane is directly dissociated to form chemisorbed surface species CH_3^* , CH_2^* , CH^* , and C^* [1,19]; (2) adsorbed formaldehyde is an important intermediate in the methane steam reforming over supported nickel catalysts [6,18]; (3) water can be dissociatively adsorbed to form surface species OH^* , H^* , and O^* [4,5]; (4) Surface species CH_xO^* can be formed by the species in (1)–(3) and they are very likely related to the formation of the precursors of CO and CO_2 [4,6,18].

Based on the kinetic nature of the methane steam reforming process, a set of elementary steps constituting the catalytic kinetics cycle may be summarized and listed in Table 1. It should be noted that the coking related to the complete dissociation of methane is not considered in this work, remaining as a topic for further simulation, in which both the rapid steps and the slow deactivation steps should be taken into account.

For each elementary step in Table 1, it is generally not practical to measure kinetic parameters, namely its rate, directly by experiments. Instead, theoretical approaches have been used to get a first approximation of the kinetic parameters of kinetic events on catalytic surface [7,20,21]. The kinetic parameters are obtained by estimating the activation energies and the pre-exponential factors on the basis of the absolute rate theories, particularly the transition theory [7,20]. For the catalytic reaction of methane steam reforming, it is convenient to estimate the energy barriers of surface steps by using bond order conservation Morse potential (BOC-MP) approach, which was theoretically developed by Shustorovich [21]. In more detail, the BOC-MP model has proven to be effective

Table 1

Mechanism of methane reforming with steam over Ni-based catalyst and kinetic parameter estimation

Mechanism model	E_a (kcal/mol)	A
$\text{H}_2\text{O} + 2^* \Rightarrow \text{OH}^* + \text{H}^*$	4	$9.4 \times 10^{-19} \text{ m}^3 \text{ s}^{-1}$
$\text{OH}^* + \text{H}^* \Rightarrow \text{H}_2\text{O} + 2^*$	10	$2.2 \times 10^{-8} \text{ m}^2 \text{ s}^{-1}$
$\text{OH}^* + ^* \Rightarrow \text{O}^* + \text{H}^*$	13	$1.2 \times 10^{12} \text{ s}^{-1}$
$\text{O}^* + \text{H}^* \Rightarrow \text{OH}^* + ^*$	28	$4.0 \times 10^{-4} \text{ m}^2 \text{ s}^{-1}$
$\text{CH}_4 + 2^* \Rightarrow \text{CH}_3^* + \text{H}^*$	8	$7.5 \times 10^{-18} \text{ m}^3 \text{ s}^{-1}$
$\text{CH}_3^* + \text{H}^* \Rightarrow \text{CH}_4 + 2^*$	13	$1.1 \times 10^{-7} \text{ m}^2 \text{ s}^{-1}$
$\text{CH}_3^* + ^* \Rightarrow \text{CH}_2^* + \text{H}^*$	24	$4.0 \times 10^{14} \text{ s}^{-1}$
$\text{CH}_2^* + \text{H}^* \Rightarrow \text{CH}_3^* + ^*$	12	$5.8 \times 10^{-8} \text{ m}^2 \text{ s}^{-1}$
$\text{CH}_2^* + \text{O}^* \Rightarrow \text{HCHO}^* + ^*$	24	$4.0 \times 10^{-5} \text{ m}^2 \text{ s}^{-1}$
$\text{HCHO}^* + ^* \Rightarrow \text{CH}_2^* + \text{O}^*$	24	$4.0 \times 10^{14} \text{ s}^{-1}$
$\text{HCHO}^* + ^* \Rightarrow \text{HCO}^* + \text{H}^*$	11	$5.0 \times 10^{11} \text{ s}^{-1}$
$\text{HCO}^* + \text{H}^* \Rightarrow \text{HCHO}^* + ^*$	17	$7.2 \times 10^{-7} \text{ m}^2 \text{ s}^{-1}$
$\text{HCO}^* + ^* \Rightarrow \text{CO}^* + \text{H}^*$	0	$1.0 \times 10^{10} \text{ s}^{-1}$
$\text{CO}^* + \text{H}^* \Rightarrow \text{HCO}^* + ^*$	24	$4.0 \times 10^{-5} \text{ m}^2 \text{ s}^{-1}$
$\text{CO}^* \Rightarrow \text{CO} + ^*$	27	$1.2 \times 10^{16} \text{ s}^{-1}$
$\text{HCO}^* + \text{O}^* \Rightarrow \text{CO}_2^* + \text{H}^*$	10	$2.2 \times 10^{-7} \text{ m}^2 \text{ s}^{-1}$
$\text{CO}_2^* + \text{H}^* \Rightarrow \text{HCO}^* + \text{O}^*$	25	$7.2 \times 10^{-5} \text{ m}^2 \text{ s}^{-1}$
$\text{CO}^* + \text{O}^* \Rightarrow \text{CO}_2^* + ^*$	22	$1.4 \times 10^{-5} \text{ m}^2 \text{ s}^{-1}$
$\text{CO}_2^* \Rightarrow \text{CO}_2 + ^*$	7	$1.0 \times 10^{13} \text{ s}^{-1}$
$\text{CO}_2^* + ^* \Rightarrow \text{CO}^* + \text{O}^*$	13	$1.2 \times 10^{12} \text{ s}^{-1}$
$\text{H}^* + \text{H}^* \Rightarrow \text{H}_2 + 2^*$	23	$5.8 \times 10^{-5} \text{ m}^2 \text{ s}^{-1}$

for treating the energetics of atomic and diatomic adsorbates on transition metal surfaces, particularly, the heat of chemisorption and activation barriers for dissociation and recombination [21–26]. Table 2 lists the results of the heats of sorption of atoms, molecule, and molecular fragments in the zero coverage within

Table 2

Heat of chemisorption (Q), total bond energy in the gas-phase (D), and chemisorption states of MSR species over (111) surfaces of nickel [15] (energies in kcal/mol)

Species	Adsorption strength	Coordination	D	Q	$D+Q$
H	Strong	$\eta^1 \mu_n$	0.0	63.0	63.0
C	Strong	$\eta^1 \mu_n$	0.0	171.0	171.0
O	Strong	$\eta^1 \mu_n$	0.0	115.0	115.0
H_2	Weak	$\eta^2 \mu_2$	104.0	6.8	110.8
CH	Strong	$\eta^1 \mu_n$	81.0	116.0	197.0
CH_2	Strong	$\eta^1 \mu_n$	183.0	82.0	265.0
CH_3	Middle	$\eta^1 \mu_3$	293.0	47.0	340.0
CH_4	Weak	$\eta^1 \mu_1$	398.0	6.0	404.0
OH	Strong	$\eta^1 \mu_n$	102.0	60.9	162.9
H_2O	Weak	$\eta^1 \mu_1$	220.0	16.5	236.5
CO	Weak	$\eta^1 \mu_1$	257.0	27.0	284.0
CO_2	Weak	$\eta^2 \mu_2$	384.0	6.5	390.5
HCO	Middle	$\eta^1 \mu_3$	274.0	49.9	323.9
HCHO	Weak	$\eta^1 \mu_1$	361.0	19.3	380.3

the BOC-MP framework. And it is possible that the pre-exponential factors for each proposed elementary step could also be estimated according to the transition state theory, which was based on the reasonable estimation normally within the magnitudes of the partition functions of all related species [7,20].

Based on the above method, the kinetic parameters for all the mechanism steps of methane steam reforming over supported nickel catalysts used in the MC simulation are also summarized in Table 1. The sticking coefficients for CH₄ and H₂O are $S_{\text{CH}_4} = 0.040$, $S_{\text{H}_2\text{O}} = 0.045$, respectively.

3. Simulation approaches

3.1. Theoretical basis

In order to describe the present MC method, it is useful to recall the physical picture of a whole catalytic process. In the starting stage, the bulk molecules collide with catalyst surface which can, as mentioned above, be represented by a two-dimensional lattice. The colliding molecules could be stucked on an active site represented by a node of such a lattice with a probability called as sticking coefficient S [7]. These stucked (sorbed) molecules can undergo surface diffusion, or reaction, or desorption from catalyst surface with the probabilities constrained by micro-kinetic rates.

For a gas–solid catalytic system, the molecule collision with catalyst surface could be described by collision theory, from which the number of molecules colliding with unit surface area in unit time could be calculated [7]:

$$F_i = \frac{P_i}{\sqrt{2\pi m_i k_B T}} \quad (1)$$

where i represents the i th component, P_i is the partial pressure of component i , m_i the molecular weight of i , k_B the Boltzmann constant, and T the absolute temperature in K.

For a given lattice with the dimension of $N \times N$, the number of colliding molecules of component i within the sampling time Δt is

$$N_{c_i} = N^2 A_s(\Delta t) \frac{P_i}{\sqrt{2\pi m_i k_B T}} \quad (2)$$

Table 3

Probabilities on the basis of scaled reaction rates of different elementary steps^a

Elementary steps	Rate equations (mol/(m ² s))	Probabilities
R-s \Rightarrow P-s	$r=k[\text{R-s}]$	$p_r=k\Delta t$
R1-s+R2-s \Rightarrow P-s+s	$r=k[\text{R1-s}][\text{R2-s}]$	$p_r=k \rho \Delta t$
R-s \Rightarrow R(g)+s	$r=k[\text{R-s}]$	$p_r=k\Delta t$
R-s+s' \Rightarrow R-s'+s	$r=k[\text{R-s}][\text{s}']$	$p_r=k \rho \Delta t$
R1-s+R2-s \Rightarrow P(g)+2s	$r=k[\text{R1-s}][\text{R2-s}]$	$p_r=k \rho \Delta t$

^a ρ is the total sites per unit surface area on the catalyst surface.

where A_s is the area of an active site on the catalyst surface in the unit of m²/site.

For the surface events involved in a kinetic process, the occurrence probabilities in the sampling time Δt can be calculated according to kinetic rates, as listed in Table 3.

It is noted that the sampling time, Δt influences the precision of the modeling results, namely very fine time resolution (Δt is very small) gives more precise curves of all the physical quantities related to surface kinetic processes during the whole simulation period. However, too many random MC steps for the system to reach equilibrium lead to computational explosion problem. The standard to choose valid sampling time for a simulation task is that the time resolution can distinguish all the surface events according to their probabilities, namely the sampling time should be chosen to meet the standard that the probabilities of all events is less than one. Thus, we have

$$(p_{r,i})_{\max} = (kC_i)_{\max} \Delta t \leq 1.0 \quad (3)$$

$$\Delta t \leq \frac{1}{(kC_i)_{\max}} \quad (4)$$

For this condition, the sampling time may be estimated by the following formula:

$$\Delta t = \frac{1}{\sum(kC_i)} \quad (5)$$

where C_i is the scaling factor for different types of the elementary steps.

3.2. Monte Carlo procedure

According to the above analysis, MC simulation can be organized as follows:

1. Initialize all the necessary memory areas to store the surface status and other simulation results, and generate the sampling time Δt and all the probabilities of surface events within Δt .
2. For the given lattice size of $N \times N$, calculate the number of molecules (Eq. (2)) colliding on the lattice within the sampling time interval Δt , which corresponds to one Monte Carlo step (MCS).
3. Randomly choose a molecule and a node for each component, which means the collision of the molecule chosen with the chosen node on the lattice. A random number RN was produced with uniform distribution over (0, 1). Then the RN was compared with the sticking coefficient S_i . If $RN \leq S_i$, the molecule i is sorbed on the node, and the lattice status should be changed to record the sorbed species, and then count the sorbed molecule; if $RN > S_i$, the molecule is not sorbed on the lattice. If this node is occupied, the molecule may react with this occupied species according to the reaction mechanism, a random number was generated to compare with the probability of this elementary step, and the status of surface is changed according to the reaction result (no change is made if no reaction occurs). Remove the molecule from the colliding list.
4. Go to (3) till all the molecules from the colliding that should collide with surface have been chosen, namely colliding list is empty.
5. Choose an occupied node of the lattice, check the type of the species on the node and check out all the events corresponding to this species, list all the probabilities of the events and put them in the array $(0, p_{i,1}, p_{i,1} + p_{i,2}, \dots, \sum_{j=1}^m p_{i,j}, \dots, 1)$, the random number RN is generated by a random generator. If RN is in $[0, p_{i,1}]$, the first event occurs, ..., if in $[\sum_{j=1}^{m-1} p_{i,j}, \sum_{j=1}^m p_{i,j}]$, the m th event occurs. Change the status of lattice and count all the molecules formed and leave the lattice.
6. Go to (5) till all the occupied nodes are checked.
7. Start the next MCS by going to (3) till the steady state is reached.
8. Statistical analysis for the simulation process, and output results.

In the above procedure, the physical quantities with real units are correlated by collision theory.

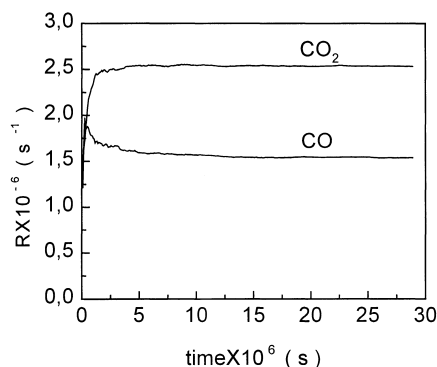


Fig. 1. Reaction rates versus simulation time ($T=800.0$ K, $P=10.0$ bar, $X_{CH_4} = 0.5$, $X_{H_2O} = 0.5$).

4. Results and discussion

In the present research, the catalytic surface is represented by a square lattice of 60×60 sites, periodic boundary conditions are used to eliminate edge effects. The simulation is carried out at the condition of the inlet of steam reformer, namely when methane conversion is zero.

Starting from the clean surface, the simulated learning curves of the formation rates of CO_2 and CO are shown in Fig. 1. The same reaction conditions with the literature [2] are adopted to compare the simulation results with the experiment data, it can be seen that the kinetic process can reach the steady state within several microseconds, and the formation rate of CO_2 (water gas shift) is higher than the net formation rate of CO, which agrees well with the literature results [2]. The variations of formation rates of CO_2 and CO with temperature are shown in Fig. 2. It

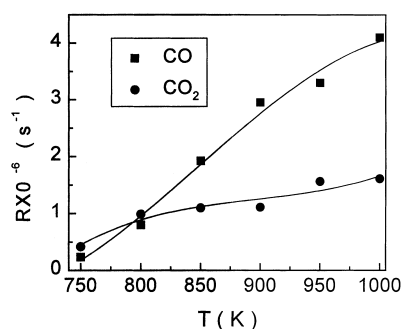


Fig. 2. Effect of temperature on reaction rates ($P=10.0$ bar, $X_{H_2O} = 0.5$, $X_{CH_4} = 0.5$).

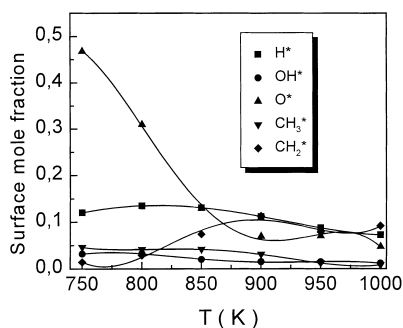


Fig. 3. Effect of temperature on surface mole fraction ($P=10.0$ bar, $X_{H_2O} = 0.5$, $X_{CH_4} = 0.5$).

can be seen that both CO and CO₂ formation rates increase with temperature increasing, and CO₂ formation rate is higher than the CO formation rate when temperature is below 800 K, and this trend is reversed when temperature is above 800 K. The reason is that mechanism of CO formation has a higher energy barrier than that of CO₂ formation as listed in Table 1. Moreover, the surface information depicted in Fig. 3 shows that the surface mole fraction of O* species decreases with temperature increasing, thus suppressing the reaction of CO* and HCO* with O* to produce CO₂*. The influence of the gas composition of reactants is shown in Fig. 4, the formation rate of CO₂ decreases as the methane to steam ratio increases, which is in good agreement with reported results [16].

In summary, the methane steam reforming mechanism is organized on the basis of the BOC-MP

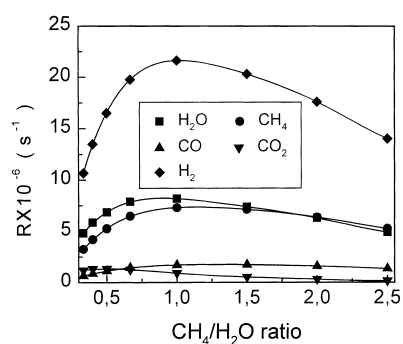


Fig. 4. Effect of CH₄/H₂O ratio on reaction rate ($P=8.0$ bar, $T=850.0$ K).

estimation of energy barriers and the reported pre-exponential factors, and the real-time Monte Carlo (RTMC) simulation approach is developed to investigate the dynamic processes on the surface. Simulation has shown that the RTMC approaches are easy to use for the description of the heterogeneous catalytic system concerning methane steam reforming. The method could reproduce the reported chemical trends observed in experiments, especially with real physical quantities and along real-time dimension, which is different from previously used MC simulation with arbitrary unit of concentration and time.

Acknowledgements

Financial support from the National Natural Science Foundation (No. 29673054) and Chinese Academy of Science is gratefully acknowledged.

References

- [1] M.A. Pena, J.P. Gomez, J.I.G. Fierro, Appl. Catal. A 144 (1996) 7.
- [2] D.W. Allen, E.R. Gehard, M.R. Likins, Ind. Eng. Chem. Process Des. Dev. 14 (1975) 256.
- [3] W.W. Akers, D.P. Camp, AIChE J. 1 (1955) 471.
- [4] J.G. Xu, G.F. Froment, AIChE J. 35 (1989) 88.
- [5] J.R.H. Ross, M.C.F. Steel, J. Chem. Soc., Faraday Trans. 1 (1973) 10.
- [6] I. Alstrup, M.T. Tavares, J. Catal. 135 (1992) 147.
- [7] J.A. Dumesic, D.F. Rudd, L.M. Aparicio, J.E. Rekoske, A.A. Trevino, The Micro-kinetic Analysis of Heterogeneous Catalysis, American Chemical Society, Washington, DC, 1993, pp. 23–53.
- [8] S.J. Lombardo, A.T. Bell, Surf. Sci. 206 (1988) 101.
- [9] S.J. Lombardo, A.T. Bell, Surf. Sci. 245 (1991) 213.
- [10] X.Y. Guo, Z.W. Liu, B. Zhong, Micropor. Mesopor. Mater. 23 (1998) 203.
- [11] X.Y. Guo, B. Zhong, S.Y. Peng, Appl. Sur. Sci. 115 (1997) 144.
- [12] R.M. Nieminen, A.P.J. Jansen, Appl. Catal. A 160 (1997) 99.
- [13] E. Klemm, J. Wang, G. Emig, Chem. Eng. Sci. 52 (1997) 3137.
- [14] L.V. Lutskevich, O.A. Tkachenko, J. Catal. 136 (1992) 309.
- [15] J.S. Turner, J. Phys. Chem. 81 (25) (1977) 2379.
- [16] J.P. Van Hook, Catal. Rev. Sci. Eng. 21 (1980) 1.
- [17] J.R. Rostrup-Nielsen, J.-H. Bak Hansen, J. Catal. 144 (1993) 38.
- [18] M.C.J. Bradford, M. Albert Vannice, Appl. Catal. A 142 (1996) 97.

- [19] I. Alstrup, M.T. Tavares, *J. Catal.* 135 (1992) 147.
- [20] V.P. Zhdanov, J. Pavlicek, Z. Knor, *Catal. Rev. Sci. Eng.* 30 (1988) 501.
- [21] E. Shustorovich, *Adv. Catal.* 37 (1990) 101.
- [22] E. Shustorovich, A.T. Bell, *Surf. Sci.* 253 (1991) 386.
- [23] E. Shustorovich, *Surf. Sci.* 163 (1985) L645.
- [24] E. Shustorovich, A.T. Bell, *Surf. Sci.* 259 (1991) L791.
- [25] E. Shustorovich, A.T. Bell, *Surf. Sci.* 248 (1991) 359.
- [26] A.T. Bell, E. Shustorovich, *J. Catal.* 121 (1990) 1.